land

MDPI

Article

Effects of Temporal and Spatial Changes in Wetlands on Regional Carbon Storage in the Naoli River Basin, Sanjiang Plain, China

Xilong Dai [1], Yue Wang [1,†], Xinhang Li [1], Kang Wang [1], Jia Zhou [1,2,*] and Hongwei Ni [1,3,*]

[1] College of Geographical Science, Harbin Normal University, Harbin 150025, China; daixilong0728@163.com (X.D.)
[2] Heilongjiang Province Key Laboratory of Geographical Environment Monitoring and Spatial Information Service in Cold Regions, Harbin Normal University, Harbin 150025, China
[3] Heilongjiang Academy of Forestry, Harbin 150081, China
* Correspondence: harbin_zhoujia@hrbnu.edu.cn (J.Z.); nihongwei2000@163.com (H.N.)
† These authors contributed equally to this work.

Abstract: The Naoli River (NLR) Basin is a crucial distribution area for wetlands in China. Investigating the link between land use changes and carbon storage in this basin is of significant importance for protecting regional ecosystems and promoting the sustainable development of the social economy. This paper uses long-term Landsat satellite images provided on the GEE (Google Earth Engine) platform and the random forest classification algorithm to create spatial distribution maps of land use in the NLR Basin from 1993 to 2022. The study analyzes the dynamic changes in wetlands in the basin over the past 30 years and employs the InVEST (Integrated Valuation of Ecosystem Services and Tradeoffs) model to explore the temporal and spatial evolution characteristics of carbon storage. The results reveal that the wetland area of the NLR Basin showed a downward trend from 1993 to 2022, with a total decrease of 1507.18 hm^2 over 30 years. During this period, the carbon storage in the NLR Basin decreased, with a cumulative loss of 1.98 $\times$ 10^7 t, mainly due to the continuous reductions in wetland and forest land. Additionally, the change in carbon storage in the basin has a strong spatial and temporal relationship with the changes in land use/cover area. The total carbon storage is positively associated with the areas of wetland, forest land, and water bodies. The conversion of wetlands into any other land type results in the reduction in carbon storage. These findings can improve our understanding of the spatial and temporal dynamics of wetlands in the NLR Basin over the past 30 years and enable us to analyze the relationship between land use changes and regional carbon storage. The results of this study have great significance for protecting the wetland ecology and regional carbon balance in the NLR Basin.

Keywords: land use and cover change; Naoli River Basin; Google Earth Engine; carbon stocks; InVEST model

Citation: Dai, X.; Wang, Y.; Li, X.; Wang, K.; Zhou, J.; Ni, H. Effects of Temporal and Spatial Changes in Wetlands on Regional Carbon Storage in the Naoli River Basin, Sanjiang Plain, China. *Land* **2023**, *12*, 1300. https://doi.org/10.3390/land12071300

Academic Editors: Zhenguo Niu, Bin Zhao, Zhaoqing Luan and Bo Guan

Received: 4 May 2023
Revised: 18 June 2023
Accepted: 22 June 2023
Published: 28 June 2023

1. Introduction

Marsh wetlands are a crucial component of the terrestrial carbon cycle [1], as they provide essential ecosystem services and play a critical role in carbon sequestration [2,3]. Although wetlands cover only 8% of the Earth's surface, they store approximately one-third of the planet's organic carbon and play a vital role in the global carbon cycle [4]. Unfortunately, wetland areas have declined by 68% since the Industrial Revolution due to climate drying and a range of unsustainable human activities [5]. As a result, it is crucial to examine the spatial and temporal changes in wetland carbon storage and develop effective wetland ecosystem carbon management strategies so as to comprehend the wetland carbon cycle process and safeguard wetland ecological environments [6,7].

As an important tool for monitoring wetland landscape patterns, remote sensing technology has the ability to quickly extract large-scale and longtime surface coverage [8,9].

The Google Earth Engine (GEE) is a cloud computing platform dedicated to processing Earth observation data from remotely sensed imagery. In the long-time-series and large-scale remote sensing exploration of the Earth, the GEE platform provides a large number of high-resolution Landsat TM/ETM+/OLI remote sensing images through dedicated cloud storage, which can access, process, and extract wetland water body information online, greatly improving the efficiency of remote sensing scholars. The Google Earth Engine is a cloud computing platform dedicated to processing Earth observation data from remote sensing images. In the long-time-series and large-scale remote sensing exploration of the earth, the GEE platform provides a large number of high-resolution Landsat TM/ETM+/OLI remote sensing images through dedicated cloud storage, which can access, process, and extract wetland water body information online, thus greatly improved the efficiency of remote sensing scholars [10]. In practice, the GEE has proven to be a powerful tool that can be used to extract wetland information [11,12].

The assessment of carbon stock in wetland ecosystems can be categorized into vegetation carbon stock and soil carbon stock [13]. Research on wetland vegetation carbon stock has progressed considerably, both domestically and internationally, with particular advancements in the estimation technology of wetland vegetation biomass utilizing 3S technology (i.e., GPS, GIS, and RS) [14,15]. In detail, wetland vegetation carbon stock mainly consists of above-ground biomass, below-ground biomass, and deadfall biomass [16]. The measurement of above-ground biomass is primarily carried out using sample field measurement methods, non-destructive estimation methods, and remote-sensing technologies. In particular, remote-sensing technology has facilitated a new approach to measuring the above-ground biomass of wetlands, offering enhanced accuracy in feature information extraction and the ability to extract long-term series of remote sensing images of wetlands. Thus, the remote-sensing techniques have been widely used to measure above-ground biomass in wetlands, despite minor errors. The methods employed to estimate the subsurface biomass of wetland plants include the digging block method, the drilling core method, the in-growth soil core method, and the micro-root zone tube method [17]. The study of deadfall carbon stock was based on quadrat sampling [18]. Jiao Yan et al. [19] explored the carbon stock of forest vegetation in Heilongjiang Province, including its dynamics, and determined that the total carbon stock of forests in the six forest inventories in Heilongjiang Province exhibited a trend of first decreasing and then increasing. Meanwhile, Long Yi et al. [20] combined the optimal GWR model with the spatial distribution of vegetation types to estimate the carbon stock of Shenzhen vegetation, with the resulting carbon stock values ranging from 1.63 to 60.95 Mg C/hm^2.

Currently, soil organic carbon is the method most commonly used to estimate soil carbon stock. Estimation methods of soil organic carbon stock include the soil type method, life zone method, and correlation method [21]. Yin Shubai et al. [22] found that organic carbon content and stock varied significantly in the soil profiles of ring-type swamp wetland, with higher levels towards the center. Their study also revealed a highly heterogeneous spatial distribution of the soil organic carbon density in the Sanjiang Plain, which was affected by land use type [23,24]. However, these traditional methods of carbon stock calculation have limitations in assessing carbon stocks on larger spatial and temporal scales due to high workloads and long sampling periods [25]. Therefore, the carbon stock assessment models are used by many experts to calculate or simulate total carbon stock changes [26]. The InVEST (Integrated Valuation of Ecosystem Services and Tradeoffs) model is a widely-used carbon stock assessment model for terrestrial ecosystems due to its low data requirements, fast operation, and high assessment accuracy [27,28].

The NLR Basin is the largest basin in the Sanjiang Plain in China and also has the largest distribution area of marsh wetlands in the country [1]. Research has revealed that natural and human factors have led to a drastic reduction in the area of marsh wetlands in the NLR Basin, which requires immediate protection [29]. It is necessary to study the carbon stock of the NLR Basin to maintain the regional carbon balance due to its significant carbon sink function. However, little attention has been paid to the study of the spatial

and temporal changes in carbon stocks in the NLR Basin wetlands, and most of the related studies are characterized by short time series, outdated research data, and low research accuracy. With the development of remote-sensing technology, satellite remote sensing data can be used to observe the wetland information of large areas and monitor its dynamic changes over time [30]. This technology provides macroscopic, high-resolution, and long-term continuous observation data of surface wetland water bodies, making it possible to study the spatial and temporal variation in the carbon stocks of wetlands in the NLR Basin.

In this study, based on the GEE platform, Landsat remote sensing image data was utilized and the random forest algorithm was employed to classify land use in the NLR Basin and analyze its spatial and temporal evolution. The obtained land use data were used with the InVEST model to analyze the spatial and temporal changes in carbon storage in the basin.

2. Materials and Methods

2.1. Study Area

The NLR Basin, which is an important marsh wetland distribution area in China, is located in the hinterland of the Sanjiang Plain in Heilongjiang Province, between 45°42′ N–47°31′ N and 131°10′ E–134°09′ E (Figure 1). The basin has an area of approximately 24,900 hm^2, with its wetland area accounting for 1/4 of the Sanjiang Plain's wetland area. It is characterized by a cold-temperate continental humid monsoon climate, with an average annual temperature of 3.3 °C and an average annual precipitation of 532 mm. Geomorphologically, the basin is characterized by high terrain in the southwest and low terrain in the northeast, and most of its rivers flow into the Ussuri River. The basin encompasses seven counties and cities, including Raohe County, Fujin City, Baoqing County, Youyi County, Jixian County, Shuangyashan City, and Qitaihe City. Agricultural activities in the basin are highly intense, and the proportion of arable land to the total area of the basin is more than 60% [31]. The NLR Basin has become the main grain-producing area of the Sanjiang Plain and an important national commercial grain base. However, four large-scale land developments have occurred in the region since 1956, resulting in the gradual fragmentation of the wetlands, drastic land use and land cover (LULC) changes, and a significant impact on the wetlands' carbon sink function. Therefore, conducting carbon-storage-related studies on the wetlands in the NLR Basin is necessary to protect the regional ecological environment.

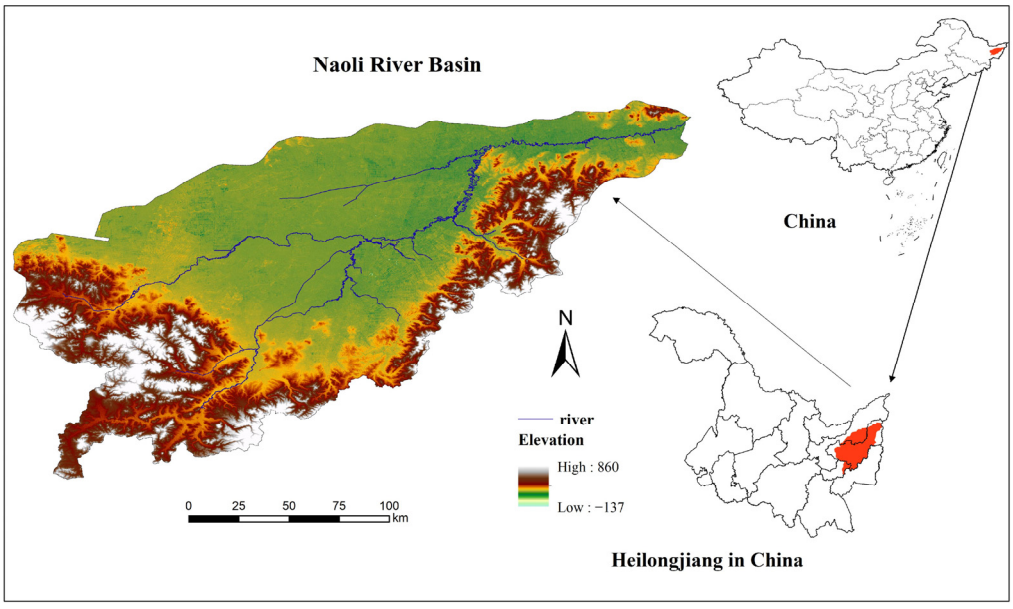

Figure 1. Location of the study area.

2.2. Data Sources

2.2.1. Data Source and Pre-Processing of the Remote Sensing Data

Based on the Landsat series satellite data provided through the GEE, all Landsat5, Landsat7, and Landsat8 satellite remote sensing images with a spatial resolution of 30 m and cloud content less than 20% during the vegetation growth period of June–October, 1993–2022, were selected for this study. After that, they were integrated, and remote sensing image datasets were constructed with geometric correction and atmospheric correction.

A series of pre-processing steps of the remote sensing images were performed to obtain high-quality remote sensing image datasets for subsequent use. The vector boundaries of the NLR basins extracted in ArcGIS were placed in GEE's personal database. The study area was cropped and mosaicked using the clip and mosaic functions. Next, the qa band (pixel_qa) generated with the mask-based C function (CFMask) algorithm was used to remove cloud layers from the remotely sensed images.

The classification features were derived using pre-processed seasonal composite images in the GEE platform, including all available spectral bands, eight spectral indices (e.g., normalized vegetation index, enhanced vegetation index, vegetation moisture content index, normalized water index, improved normalized difference water index, normalized building index, naked soil index, and remotely sensed building land index) with the abbreviations NDVI, EVI, LSWI, MNDWI, NDBI, BSI, and IBI, in that order. The texture means based on the gray-scale covariance matrix (GLCM) and incorporating topographic features derived from the SRTM data (including the elevation, slope, slope orientation, and hill shading) were used as auxiliary classification data.

2.2.2. Sample Point Selection and Validation

In accordance with the Classification of Land Use Status, representative land cover categories were selected based on the status quo and characteristics of land use in the study area. These categories were primarily classified into five types: water, woodland, wetland, cropland, and build. To ensure an accurate selection of sample points, a buffer zone of 60 m was created outward for each sample point, and all points within this area were considered as the sample set. The sample points were chosen for each year using the visual interpretation method. The sample points were randomly divided into two sets of 70% and 30%, respectively, for classifier training and accuracy verification.

2.2.3. Carbon Density Data

The carbon density data used in this study mainly referred to previous research results, and priority was given to data measured in the field near the Sanjiang Plain. If the comprehensiveness of the data was not sufficient, data measured and compiled in the literature of the same climatic zone as the study area were selected, and the data were corrected as needed. The carbon density data of the NLR Basin are shown in Table 1.

Table 1. Carbon density of different land types in the NLR Basin (t/ha).

Land Type	C_{above}	C_{below}	C_{soil}	C_{dead}	C_{total}	Reference
Water	8.72	2.21	23.01	0	33.94	[32,33]
Woodland	11.46	31.32	173.9	2.02	218.7	[33,34]
Wetland	45.11	92.71	147.84	0	258.66	[24,35]
Cropland	10.1	26.8	147	0	183.9	[32,33]
Build	8.75	4.39	27.78	1.16	41.68	[32,33]

C_{total} represents the total carbon storage; C_{above} represents the aboveground carbon storage of vegetation; C_{below} represents the underground carbon storage of vegetation; C_{soil} represents soil carbon storage; C_{dead} represents the carbon storage of dead organic matter.

2.3. Method

The flow chart of the method used in this study is shown in Figure 2.

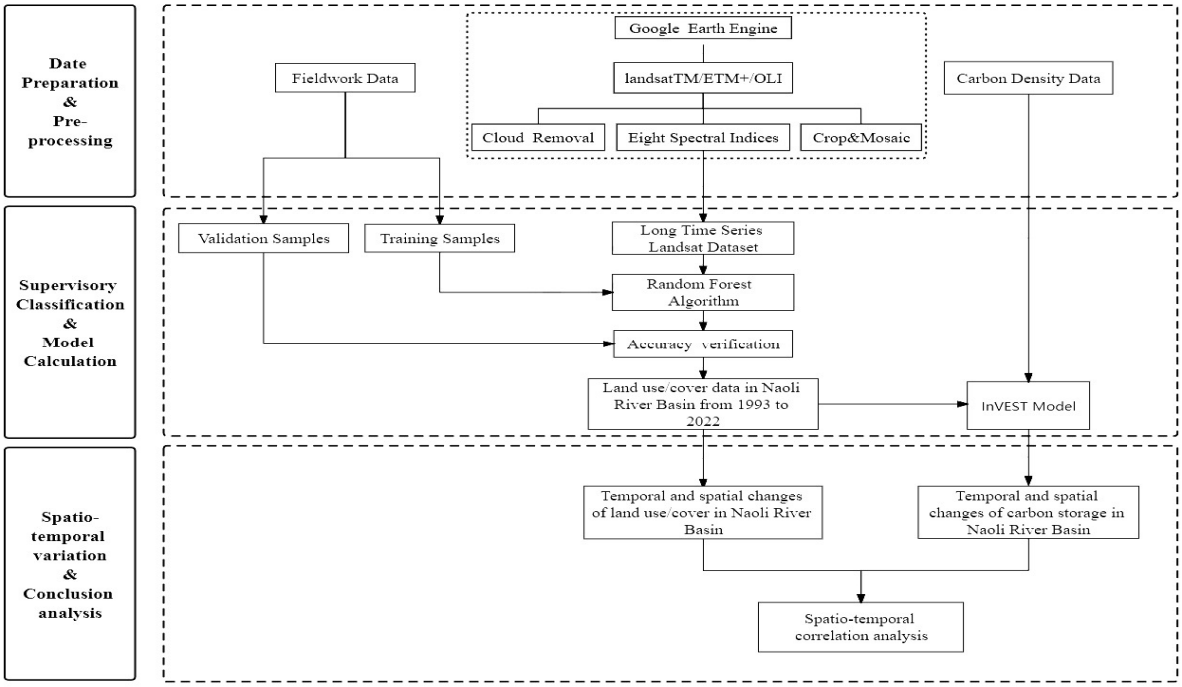

Figure 2. The flow chart of the method used in this study.

2.3.1. Random Forest Algorithm

Random forest (RF) is a machine learning algorithm that consists of multiple classification decision trees [36]. The algorithm works as follows: assuming that there are several datasets to be trained, a random sampling method is used to extract samples from the selected data through visual interpretation. The extracted samples form the training sample set of each decision tree. The training samples account for approximately two-thirds of the original data, while the remaining one-third are used as test data to form a test decision tree. The prediction category of the sample is determined through voting based on the decision tree nodes, and the classification result is finally obtained. Compared to other neural network calculation algorithms, the RF algorithm has several advantages, including a high calculation accuracy, shorter model training time, and the ability to determine the importance of variables in the model. Therefore, this method is widely used in classification research.

2.3.2. Precision Evaluation Method

The accuracy of validation was determined using the confusion matrix and the GEE platform for visual interpretation of the sample points in the NLR Basin LULC. The overall accuracy and Kappa coefficient were then calculated. Overall accuracy is a measure of the algorithm's effectiveness and is calculated by determining the number of correctly classified samples as a percentage of the total number of validated samples. The Kappa coefficient, on the other hand, measures the degree of agreement between the predicted values and the ground truth data [37]. To obtain the accuracy evaluation index, the mixing matrix was calculated using the validation samples through the ImageCollection.errorMatrix (actual, predicted, order) function of the GEE platform, which provides the overall accuracy (OA) and Kappa coefficient.

2.3.3. InVEST Model

The carbon storage module in the InVEST (Integrated Valuation of Ecosystem Services and Tradeoffs) model divides the carbon storage of the ecosystem into four basic carbon pools: aboveground biological carbon (carbon in all surviving plant materials above the soil), underground biological carbon (carbon present in the plant living root system), soil

carbon (organic carbon distributed in organic soil and mineral soil), dead organic carbon (carbon in litter, inverted or standing dead trees). The calculation formula is as follows:

$$C_{total} = C_{above} + C_{below} + C_{soil} + C_{dead} \quad (1)$$

where C_{total} represents the total carbon storage; C_{above} represents the aboveground carbon storage of vegetation; C_{below} represents the underground carbon storage of vegetation; C_{soil} represents soil carbon storage; and C_{dead} represents the carbon storage of dead organic matter.

2.3.4. Correlation Analysis

In this study, wetland area was regarded as a continuous variable with a non-normal distribution, and linear regression analysis in Origin 2022 was used to explore the correlation between the wetland area and carbon storage in the NLR Basin.

3. Results

3.1. Analysis of LULC Classification Mapping Results for the NLR Basin

The RF algorithm on the GEE platform was used to obtain the land use type data of the NLR Basin for five-year intervals from 1993 to 2022, and its overall accuracy and Kappa index were above 90% (Table 2), achieving a relatively good classification effect. The classification results are shown in Figures 3 and 4.

Table 2. Classification overall accuracy and Kappa coefficient.

	1993	1998	2003	2008	2013	2018	2022
Overall accuracy	96.18%	96.74%	96.34%	97.10%	97.30%	97.63%	96.73%
Kappa	0.9449	0.9532	0.9456	0.9578	0.9607	0.9619	0.9473

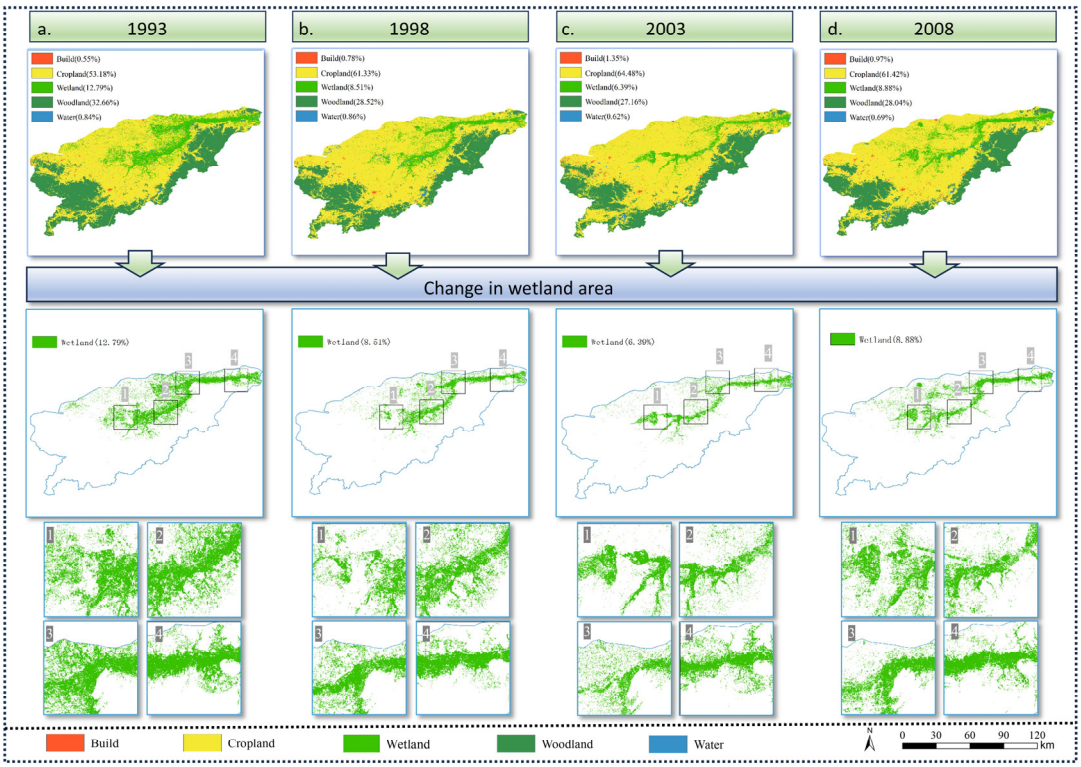

Figure 3. Five-year land use change map of the NLR Basin from 1993 to 2022, in which (**a**–**d**) show the land use distribution maps of 1993, 1998, 2003, and 2008, respectively, '1, 2, 3, 4' are typical areas of the NLR Basin.

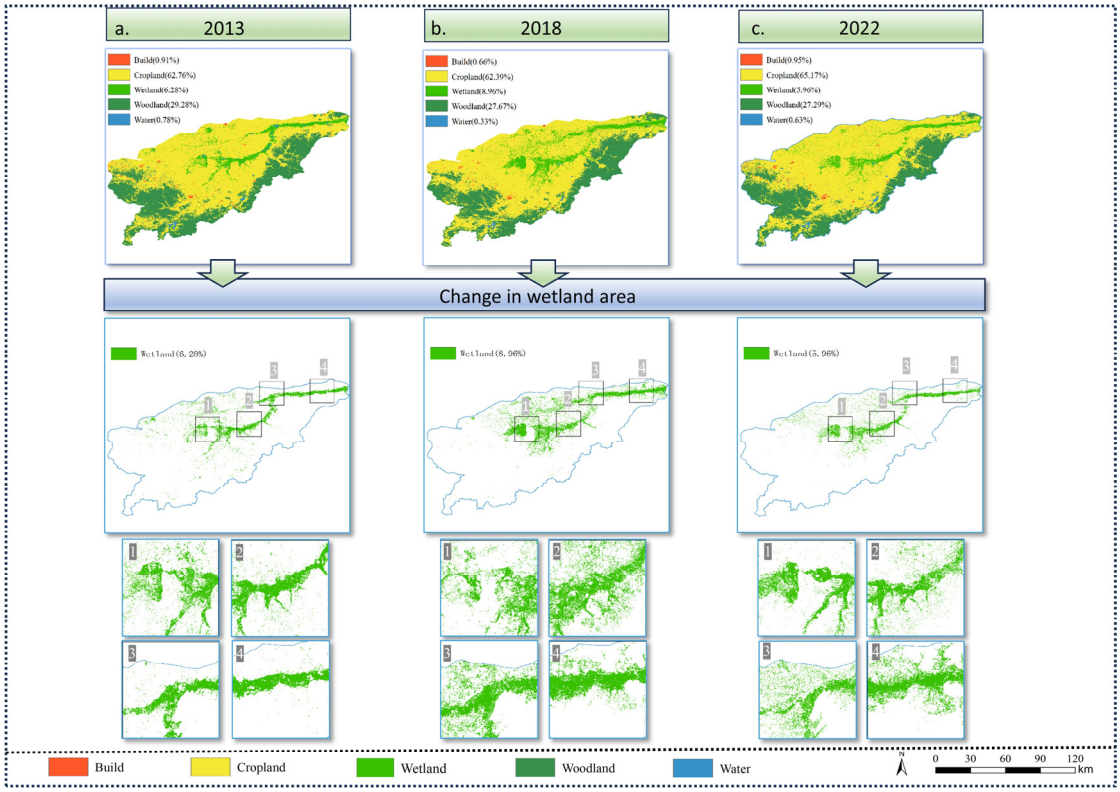

Figure 4. Five-year land use change map of the NLR Basin from 1993 to 2022, in which (**a**–**c**) show the land use distribution maps of 2013, 2018, and 2022, respectively, '1, 2, 3, 4' are typical areas of the NLR Basin.

3.2. Spatial and Temporal Changes in LULC in the NLR Basin

It is evident from Figure 5 that the structure and distribution of wetlands in the NLR Basin underwent significant changes from 1993 to 2022, with a general decreasing trend despite fluctuations in the wetland area. Specifically, the wetland area reduced from 2823.96 hm^2 in 1993 to 1316.78 hm^2 in 2022, with 1413.69 hm^2 lost from 1993 to 2003; 24.11 hm^2 lost from 2003 to 2013; and 69.36 hm^2 lost from 2013 to 2022. The past three decades saw the wetland area decrease by 1507.18 hm^2. Figures 5 and 6 reveal that cultivated land and water bodies are the primary conversion types of wetlands. Overall, from 1993 to 2022, around 416.42 hm^2 of wetland area was converted into cultivated land, and 38.39 hm^2 was converted into water.

From 1993 to 2022, the area of cultivated land in the NLR Basin exhibited a steady increase, rising from 11,744.47 hm^2 in 1993 to 14,393.49 hm^2 in 2022. Conversely, the forest land area decreased from 7212.35 hm^2 in 1993 to 6027.28 hm^2 in 2022. While the area of water and construction land varied during this time, there was no clear trend. This indicates that the expansion of cultivated land has led to the degradation of wetland and forest land in the NLR Basin, which necessitates urgent protection.

From a spatial perspective, the wetlands in the NLR Basin are primarily distributed near the banks of the NLR and the Qixing River in a discrete surface pattern around the water bodies. In 1993, the wetlands in the NLR Basin were extensively distributed in the central and northeastern areas of the basin. However, by 2003, the wetland area had significantly decreased, particularly at the confluence of the NLR and the Qixing River. Although the wetland area continued to decline in 2013, the rate of change stabilized. Although the wetland area had recovered somewhat by 2022, it remained significantly smaller than the 1993 level, indicating an obvious trend of fragmentation.

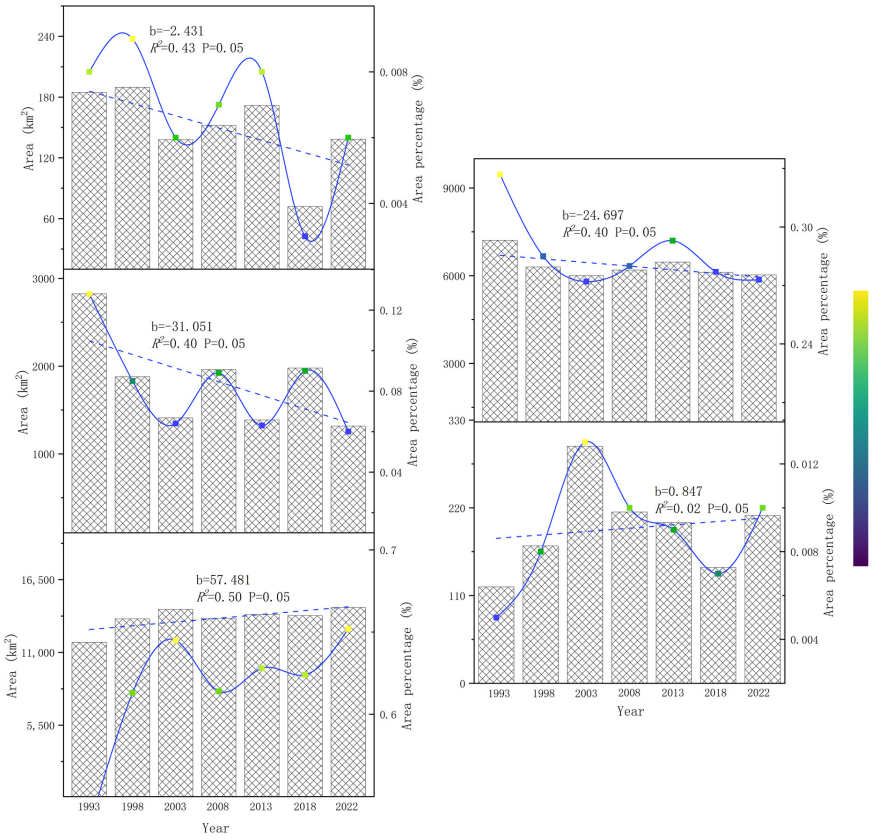

Figure 5. (km^2) Changes in area of different land use types in the NLR Basin from 1993 to 2022. The columns represent the area percentages of different LULC types, and the dashed lines represent the linear fits of different LULC areas in the four periods.

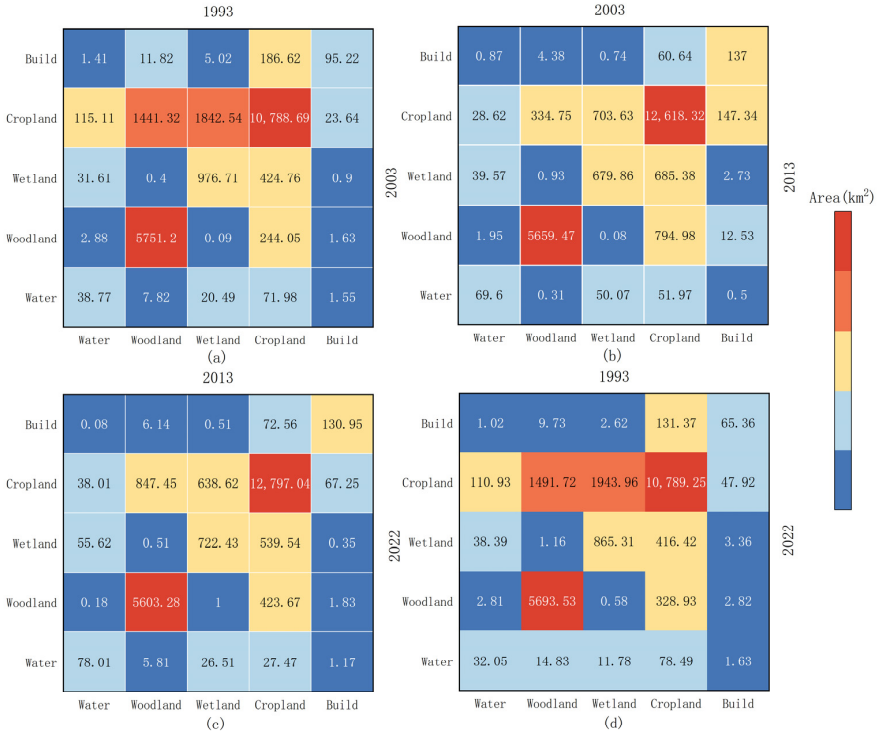

Figure 6. Heat map of land use transfer in the NLR Basin: (**a**) 1993–2003; (**b**) 2003–2013; (**c**) 2013–2022; (**d**) 1993–2022.

From 1993 to 2022, the distribution of cultivated land in the NLR Basin was concentrated in large areas in the western and central regions of the basin. During this period, the cultivated land continued to encroach on forest and wetland areas, resulting in an increase in the total area of cultivated land in the basin. The forest land in the NLR Basin was mainly distributed in the southeastern and western regions of the basin during the same period. However, due to the encroachment of cultivated land, the distribution of forest land became increasingly fragmented. There were no significant spatial changes in the water or built-up land during this period.

3.3. Spatial and Temporal Changes in LULC Carbon Storage in the NLR Basin

Using the carbon storage module of the InVEST model, we estimated the carbon storage of the NLR Basin in seven periods between 1993 and 2022, including 1993, 1998, 2003, 2008, 2013, 2018, and 2022 (Figure 7). The carbon storage in the study area first decreased and then increased from 1993 to 2022. Overall, the carbon storage in the basin decreased by 1.98×10^7 t from 1993 to 2022, with the most significant decline observed during 1993–2003, resulting in a decrease of 2.03×10^7 t. This decrease was mainly due to the reduction in the wetland and forest land area and the increase in the cultivated land area. However, from 2003 to 2022, the carbon storage in the basin showed a slight upward fluctuation, increasing by 0.05×10^7 t. This increase was mainly due to the implementation of the policy of returning farmland to forest land and returning farmland to wetland, which helped to restore the area of forest wetland.

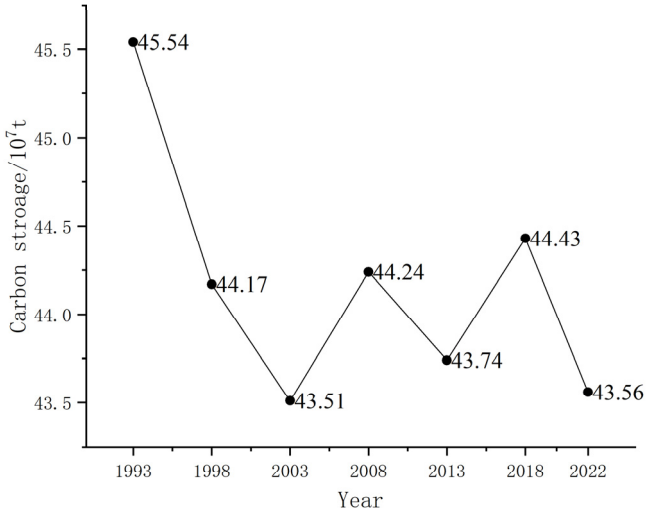

Figure 7. Carbon storage and trend in the study area (10^7 t) in different years.

From the perspective of land use types, the carbon storage of wetlands in the NLR Basin showed a decreasing trend from 1993 to 2022 (Table 3). Over this period, wetland carbon storage decreased by 4.27×10^7 t, declining from 8.12×10^7 t in 1993 to 3.85×10^7 t in 2022. Moreover, the carbon storage of forest land decreased from 15.77×10^7 t in 1993 to 13.18×10^7 t in 2022, while the carbon storage of cultivated land increased from 21.54×10^7 t in 1993 to 26.39×10^7 t in 2022. The carbon storage of construction land and water bodies did not change significantly during this period.

From a spatial distribution perspective, the carbon storage in the NLR Basin exhibits significant spatial heterogeneity, as shown in Figure 8. The areas with high carbon storage values are primarily located in the eastern and southern regions of the study area, where wetlands and woodlands are the main land use types. These regions have a large vegetation area and a high carbon storage capacity. From 1993 to 2022, the carbon storage in the study area initially decreased and then increased, with an average carbon storage of 44.17×10^7 t over many years. The staggered distribution of different land use types in the study area resulted in a staggered carbon storage distribution.

Table 3. Carbon storage according to land use type in the NLR Basin from 1993 to 2022 (10^7 t).

Year	Water	Woodland	Wetland	Cropland	Build	Total
1993	0.06	15.77	8.12	21.54	0.05	45.54
1998	0.07	13.77	5.41	24.85	0.07	44.17
2003	0.05	13.12	4.09	26.13	0.12	43.51
2008	0.05	13.54	5.67	24.89	0.09	44.24
2013	0.06	14.14	4.02	25.43	0.09	43.74
2018	0.02	13.36	5.70	25.29	0.06	44.43
2022	0.05	13.18	3.85	26.39	0.09	43.56

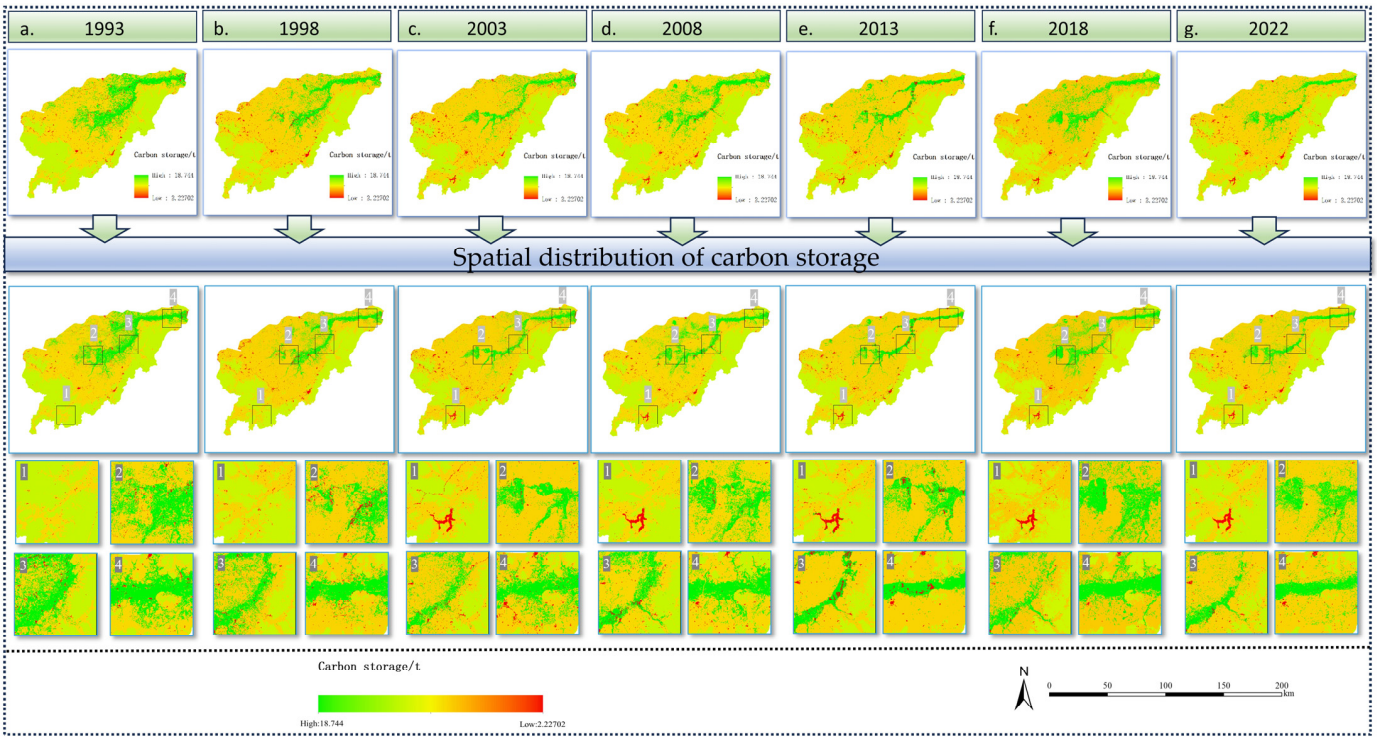

Figure 8. Spatial distribution of carbon storage in the NLR Basin: (**a**) 1993; (**b**) 1998; (**c**) 2003; (**d**) 2008; (**e**) 2013; (**f**) 2018; (**g**) 2022, '1, 2, 3, 4' represents the typical area of carbon storage change in NLR Basin.

From 1993 to 2003, the spatial distribution of carbon storage in the study area exhibited considerable variability, with an average of 44.41 × 10^7 t. The regions with high carbon storage were predominantly situated in the eastern and southern parts of the study area, while the central region demonstrated low carbon storage, with sporadic, dispersed areas having the lowest storage. The decrease in total carbon storage from 2003 to 2013 can be attributed to several factors, including the expansion of cultivated land, a decline in wetland and forest areas, and a reduction in the average annual precipitation. The period between 2013 and 2022 showed a decline in high-value areas of carbon storage in the eastern and southern parts of the study area, as compared to 1993–2003. The cultivated land area in the central region was identified as the primary region for low carbon storage during this period.

In order to better depict the changes in carbon storage in the study area, a spatial change map of carbon storage was constructed for the period of 1993–2022 by reclassifying the difference value of each decade. The spatial variation in carbon storage during this period was classified into three categories: reduction, no significant change, and increase, as shown in Figure 9. The spatial variation in carbon storage showed the characteristics of large aggregation and sporadic distribution. During the period of 1993–2003, the spatial variation in carbon storage was intense, with the increase in carbon storage mainly concentrated in

the central and eastern regions of the basin. However, the carbon storage showed a sporadic distribution and mainly exhibited a decreasing trend. The area with a significant reduction in carbon storage was concentrated in the central region of the basin, where the carbon storage changed dramatically. In contrast, the spatial variation in carbon storage during the periods of 2003–2013 and 2013–2022 was relatively stable, with the area of carbon storage change mainly being concentrated in the central part of the basin near the banks of the NLR and Qixing River. The carbon storage in the other regions remained unchanged. Overall, the change in carbon storage in this basin from 1993 to 2022 was intense. The area with significant changes in carbon storage was mainly concentrated on both sides of the NLR and the Qixing River. The establishment of the NLR National Nature Reserve and the completion of water conservancy projects such as Longtou Bridge have influenced the carbon stocks in the central and northeastern regions of this region and the upper reaches of the basin to varying degrees. In addition, the expansion of cultivated land has led to the conversion of wetlands and woodlands into paddy fields and dry land, causing sporadic reductions in carbon storage in the eastern and central regions of the basin.

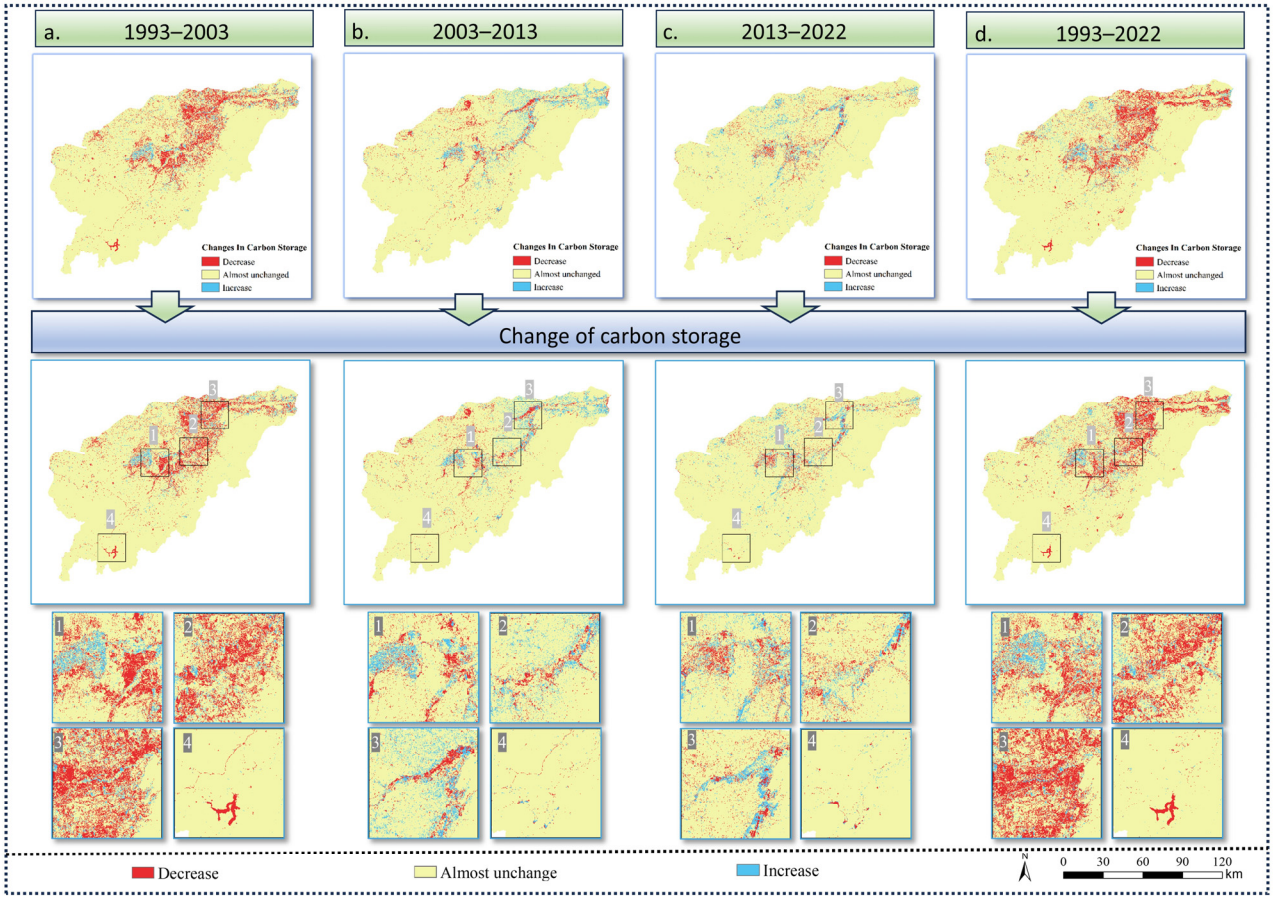

Figure 9. Changes in carbon storage in the NLR Basin: (**a**) 1993–2003; (**b**) 2003–2013; (**c**) 2013–2022; (**d**) 1993–2022, '1, 2, 3, 4' represents the typical area of carbon storage change in NLR Basin.

3.4. The Effect of LULC Change on Carbon Storage in the NLR Basin

Combining Figures 8 and 9, the carbon storage in the NLR Basin is closely related to the change in LULC. The change in LULC is one of the reasons for the change in carbon storage in the NLR Basin. Table 4 shows that LULC changes from 1993 to 2022 resulted in a decrease in carbon storage of approximately 626.02 $\times$ 10^5 t. Specifically, the conversion of wetlands into other land types resulted in a significant reduction in carbon stocks, with a total loss of 437.5 $\times$ 10^5 t. Additionally, the conversion of forest land also reduced carbon storage by 336.21 $\times$ 10^5 t. However, the conversion of cultivated land, water bodies, and

construction land increased carbon storage, although the overall trend was still decreasing. The conversion of water bodies into other land types, forest land into wetlands, and cultivated land into woodland and wetland, as well as the conversion of construction land into wetland, woodland, and cultivated land, were beneficial for the increase in carbon storage. In contrast, the conversion of wetlands and forest land into other land types was not conducive to carbon storage increase. The main reason for the decrease in carbon storage was the conversion of wetland and forest land into cultivated land, resulting in a loss of 772.18 $\times$ 10^5 t.

Table 4. Change in carbon storage caused according to land use type conversion from 1993 to 2022.

1993–2022	Area/km^2	Change of Carbon Storage/10^5 t	Subtotal/10^5 t
Water–woodland	2.81	0.51	30.72
Water–wetland	38.39	5.24	
Water–cropland	110.93	24.93	
Water–build	1.02	0.04	
Woodland–water	14.83	−0.38	−336.21
Woodland–wetland	1.16	0.15	
Woodland–cropland	1491.72	−335.27	
Woodland–build	9.73	−0.71	
Wetland–water	11.78	−0.3	−437.5
Wetland–woodland	0.58	−0.10	
Wetland–cropland	1943.96	−436.91	
Wetland–build	2.62	−0.19	
Cropland–water	78.49	−2.04	105.29
Cropland–woodland	328.93	60.13	
Cropland–wetland	416.42	56.88	
Cropland–build	131.37	−9.68	
Build–water	1.63	−0.04	11.68
Build–woodland	2.82	0.51	
Build–wetland	3.36	0.45	
Build–cropland	47.92	10.76	

Overall, the carbon storage of wetlands and forest lands decreased, while the carbon storage of cultivated land, water bodies, and construction land increased. Among these types, wetland carbon storage decreased the most, while cultivated land carbon storage increased the least. The order of the carbon storage values of different LULC types in the total carbon storage in the study area was as follows: cultivated land (60.57%) > forest land (30.25%) > wetland (8.85%) > construction land (0.02%) > water body (0.01%). Wetlands, with an area of only 5.96%, accounted for 8.85% of the carbon storage, making them an important carbon pool in the NLR Basin. Although the area of forest land is declining, it still accounts for a large proportion of carbon storage, making it the main carbon pool in the study area.

In order to explore the relationship between land use change and total carbon storage in the study area, we calculated the correlation between the LULC area change and total carbon storage from 1993 to 2022. Figure 10 shows that the total carbon storage in the study area is positively correlated with the area of wetland and forest land, since the wetland and forest land have a high carbon density, and large carbon sequestration in soil, which significantly affects regional carbon storage. Conversely, the area of cultivated land is negatively correlated with total carbon storage. Although the area of cultivated land has increased, it has mainly been converted from wetlands and woodlands with high carbon storage, resulting in a negative correlation with total carbon storage. The correlation between the area of the build and water categories and the total carbon stock is not clear. It is possible that other factors have a significant effect on the carbon stocks of these two types of land.

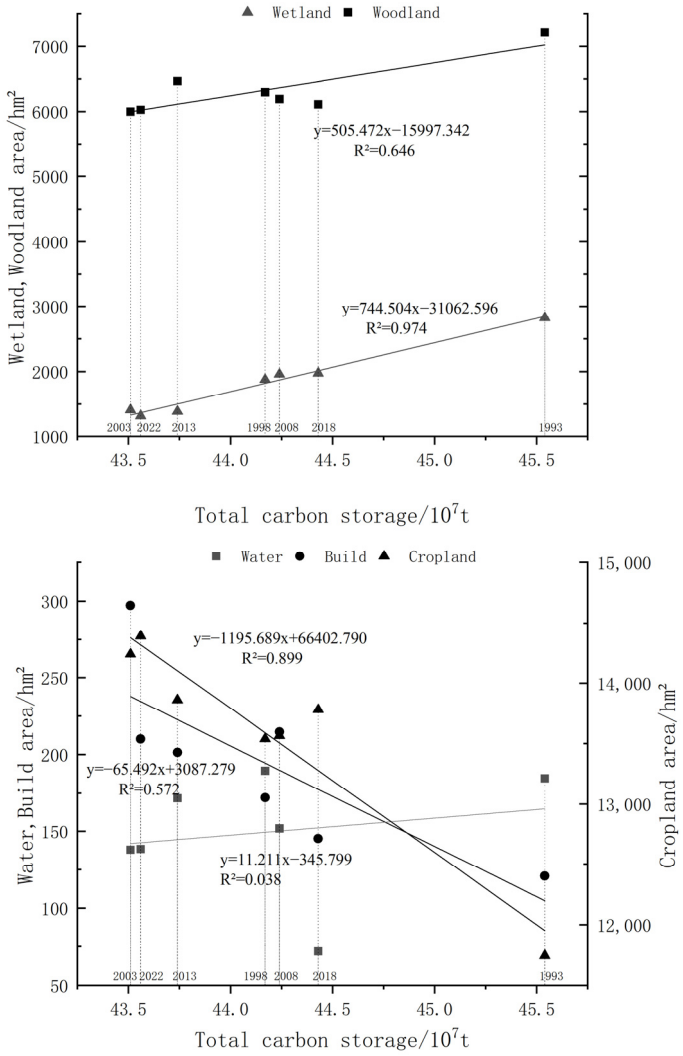

Figure 10. Relationship between land use and total carbon storage.

4. Discussion

4.1. Spatial and Temporal Changes in Wetlands in the NLR Basin Based on the GEE Platform

In this study, the RF algorithm in the GEE platform was used to obtain the land use type data of the NLR Basin at five-year intervals from 1993 to 2022. The overall accuracy and Kappa coefficient were above 90%, achieving a relatively good classification result. Due to the continuous innovation of machine learning methods, many scholars have achieved good accuracy using machine learning algorithms for wetland mapping [38–40]. The results of this paper provide a new method for wetland mapping. Nevertheless, higher-resolution data could be used to further improve the accuracy of mapmaking in the future remote-sensing monitoring of wetlands.

In this study, the LULC distribution map of the NLR Basin from 1993 to 2022 was obtained through the GEE platform. The results showed that the wetlands in the NLR basin showed a degradation trend, which was consistent with the results of previous studies, and the marsh wetlands in the NLR basin were severely degraded in the last 40 years due to the influences of various factors [41]. Natural and anthropogenic factors have contributed to the gradual loss of wetlands in the region [42]. Specifically, between 1993 and 2022, the wetland area decreased by 1507.18 hm^2, with 416.42 hm^2 being converted to cultivated land. The expansion of cropland is a key factor in wetland degradation. In line with previous research, human farming activities are the main driver of wetland area retreat in the NLR basin [43]. Between 1993 and 2003, the devaluation of several dryland crops led to their conversion into

paddy fields, resulting in wetland area shrinkage. Simultaneously, state-led development prioritized drainage network and road system construction, further exacerbating wetland degradation [44]. While the area of wetlands continued to exhibit a degradation trend from 2003 to 2013 and from 2013 to 2022, the rate slowed down. This can be attributed to the impacts of reduced river supplementary water, climate change, and small-scale illegal reclamation, which represent the results of both natural and anthropogenic factors.

4.2. Effects of Temporal and Spatial Variation in Wetlands on Carbon Storage in the NLR Basin

The change in LULC is one of the reasons for the change in the soil organic carbon content; meanwhile, the area where the LULC is changed is also the area where the carbon stock is drastically changed [45]. From 1993 to 2022, the carbon storage in the NLR Basin showed a trend of decline–rise–fluctuation, shifting from 45.54×10^7 t in 1993 to 43.56×10^7 t in 2022. During this time, the overall fluctuation in carbon storage in the region was considerable. The substantial expansion of cultivated land led to the encroachment of high-carbon wetlands and woodlands, resulting in a significant loss of carbon storage that is consistent with the marked shrinkage of these areas. Our results reveal the impact of LULC on regional carbon stocks, which is consistent with the findings of previous studies. LULC is one of the causes of changes in ecosystem carbon stocks [46]. In light of these results, we recommend that the NLR Basin prioritize efforts to restore farmland to wetland and forest land, protect the ecosystem, improve the compensation mechanism for farmland restoration, enhance the carbon sequestration capacity of wetland forest ecosystems, and promote local sustainable development.

According to previous research, many scholars have evaluated the impacts of wetland changes on carbon storage in the Sanjiang Plain, consistent with the findings of this study. The conversion of woodland and swampy wetland into cropland leads to a decrease in vegetation carbon stocks, and the conversion of cropland into woodland and swampy wetland leads to an increase in vegetation carbon stocks [47]. From 1993 to 2022, the wetland area in the NLR Basin fluctuated after a sharp decline, which was highly correlated with the change in carbon storage in the study area. Figure 10 demonstrates that the total carbon storage in the study area exhibited a significant positive correlation with changes in the wetland area. In addition, the total carbon storage showed a significant positive correlation with forest land and a negative correlation with cultivated land, which is consistent with the findings of other scholars. Wang Lili et al. [48] found that the expansion of cultivated land reduces the organic carbon storage of wetland soil, and the return of farmland to wetland is conducive to the fixation of soil organic carbon and the increase in regional carbon storage.

In addition, studies from many countries have revealed the relationship between LULC changes and carbon stocks [49]. For instance, Xiaoqing Chang et al. [50] analyzed the impacts of changes in LUCC on terrestrial carbon stocks in China from 2000 to 2018, and the results showed that LUCC had a significant impact in increasing the terrestrial carbon pool sink in China. Similarly, M. Maanan et al. [51] assessed the impacts of LULC changes on carbon stocks in northwestern Morocco using the InVEST model, and the results showed that the total carbon stocks increased from 4.81 TgC in 1996 to 4.98 TgC in 2017, with the largest impact of LULC on carbon stocks. This is consistent with the results of the NLR basin, where the change in LULC was one of the relevant factors for the change in carbon stock. Shuqing Zhao et al. [52] studied the relationship between LUCC and carbon sink in the southeastern U.S. from 1992 to 2050, showing that urban expansion affected the carbon sink function of the region, leading to the decrease in the regional carbon stock. In general, the impact of LULC changes on regional carbon stocks is a long-term process; thus, policy makers should fully consider this factor when formulating ecological conservation policies.

4.3. Deficiencies and Prospects

Based on the GEE platform, the Landsat remote sensing image data were utilized, and the RF algorithm was employed to classify land use in the NLR Basin and analyze its

spatial and temporal evolution. The obtained land use data were used with the InVEST model to analyze the spatial and temporal changes in carbon storage in the basin. However, this study has some limitations.

Firstly, the NLR Basin, located in the Sanjiang Plain of Heilongjiang Province, is characterized by widely distributed marsh wetlands, a complex geography, and diverse land use types. Due to the limitations of some technical measures, this study only selected five representative land types, neglecting the divisions of grassland, swamp, and unused land. Therefore, in future studies, land use classification should include grassland, swamp, and unused land divisions in remote sensing image analysis. Moreover, due to the lack of field survey data, the accuracy verification of this classification is incomplete.

Secondly, carbon density data that were mainly derived from previous studies were used when calculating the carbon storage of the NLR Basin using the InVEST model. While the selected carbon density data were mostly derived from the Sanjiang Plain, which is not geographically distant from the NLR Basin, the InVEST model disregarded differences in the vegetation types and growth conditions of the same land type, as well as the changes in carbon density values over time. Therefore, in future research, land types should be classified more precisely and accurate carbon density data should be obtained through extensive soil sampling in order to accurately measure carbon storage.

5. Conclusions

The main conclusions of this article are as follows:

(1) Over the past 30 years (1993–2022), the overall trend of the wetland area in the Flexi River Basin has decreased, with a total reduction of 1507.18 hm^2. The wetlands were primarily concentrated in the central and northeastern parts of the study area, in a strip pattern on both sides of the NLR and Qixing Rivers. The main land use transfer observed was the conversion of wetlands into cropland, accounting for 8.8% of the total study area.

(2) From 1993 to 2022, the carbon storage of the NLR Basin showed a downward trend followed by a fluctuating upward trend, with an overall decrease of 1.98×10^7 t. The wetland distribution in the central and eastern regions had higher carbon storage compared to the other areas. The total carbon storage was positively correlated with the area of wetland, forest land, and water bodies. Any conversion of wetland into other land types would result in a reduction in carbon storage. Wetlands accounted for 8.85% of the carbon storage despite occupying only 5.96% of the total area in the NLR Basin. This highlights the significance of wetlands as an important carbon pool.

(3) In this study, we showed that the wetlands in the NLR Basin are significant carbon sinks, with minimal human activity and abundant natural vegetation and biodiversity. The implementation of strict natural resource protection policies is necessary to optimize the land use structure and promote sustainable development in the NLR Basin.

Author Contributions: Conceptualization, X.D. and J.Z.; methodology, X.D.; software, X.D.; validation, Y.W., J.Z. and H.N.; formal analysis, X.D.; investigation, X.D.; resources, X.D.; data curation, Y.W., J.Z. and H.N.; writing—original draft preparation, X.D.; writing—review and editing, J.Z.; visualization, X.D. and K.W.; supervision, X.L., J.Z. and H.N.; project administration, J.Z. and H.N.; funding acquisition, J.Z. All authors have read and agreed to the published version of the manuscript.

Funding: This study was financially supported by the Heilongjiang Provincial Scientific Research Institutes Scientific Research Business Fee Project (CZKYF2021-2-A005), the Innovative Research Project for Postgraduate of Harbin Normal University (HSDSSCX2019-02).

Data Availability Statement: Not applicable.

Acknowledgments: The authors gratefully acknowledge the editors and reviewers for offering suggestions and comments on this paper.

Conflicts of Interest: The authors declare no conflict of interest.

References

1. Liu, Z.; Lu, X.; Yonghe, S.; Zhike, C.; Wu, H.; Zhao, Y. Hydrological evolution of wetland in Naoli River Basin and its driving mechanism. *Water Resour. Manag.* **2012**, *26*, 1455–1475. [CrossRef]
2. Li, J. The spatial distribution of soil organic carbon density and carbon storage in Baiyangdian wetland. *Acta Ecol. Sin.* **2020**, *40*, 8928–8935.
3. Min, R.; Haibo, W. Landscape Patterns Change of the Heihe Wetland of Zhangye and Its Value Assessment of Carbon Storage in Recent 15 Years. *J. Arid. Meteorol.* **2020**, *38*, 828.
4. Yu, Z.; Loisel, J.; Brosseau, D.P.; Beilman, D.W.; Hunt, S.J. Global peatland dynamics since the Last Glacial Maximum. *Geophys. Res. Lett.* **2010**, *37*, L13402. [CrossRef]
5. Mu, C.; Wang, B.; Lu, H.; Bao, X.; Cui, W. Carbon storage of natural wetland ecosystem in Daxing'anling of China. *Acta Ecol. Sin.* **2013**, *33*, 4956–4965.
6. Whiting, G.J.; Chanton, J.P. Greenhouse carbon balance of wetlands: Methane emission versus carbon sequestration. *Tellus B* **2001**, *53*, 521–528. [CrossRef]
7. Mitsch, W.J.; Nahlik, A.; Wolski, P.; Bernal, B.; Zhang, L.; Ramberg, L. Tropical wetlands: Seasonal hydrologic pulsing, carbon sequestration, and methane emissions. *Wetl. Ecol. Manag.* **2010**, *18*, 573–586. [CrossRef]
8. Wang, H.; Ma, M.; Geng, L. Monitoring the recent trend of aeolian desertification using Landsat TM and Landsat 8 imagery on the north-east Qinghai–Tibet Plateau in the Qinghai Lake basin. *Nat. Hazards* **2015**, *79*, 1753–1772. [CrossRef]
9. Hai-Bo, W.; Ming-Guo, M. A Review of Monitoring Change in Lake Water Areas Based on Remote Sensing. *Remote Sens. Technol. Appl.* **2010**, *24*, 674–684.
10. Sreekanth, P.; Krishnan, P.; Rao, N.; Soam, S.; Srinivasarao, C. Mapping surface-water area using time series landsat imagery on Google Earth Engine: A case study of Telangana, India. *Curr. Sci.* **2021**, *120*, 1491–1499. [CrossRef]
11. Yin, H.; Hu, Y.; Liu, M.; Li, C.; Chang, Y. Evolutions of 30-year spatio-temporal distribution and influencing factors of Suaeda salsa in Bohai Bay, China. *Remote Sens.* **2022**, *14*, 138. [CrossRef]
12. Zhao, F.; Feng, S.; Xie, F.; Zhu, S.; Zhang, S. Extraction of long time series wetland information based on Google Earth Engine and random forest algorithm for a plateau lake basin—A case study of Dianchi Lake, Yunnan Province, China. *Ecol. Indic.* **2023**, *146*, 109813. [CrossRef]
13. Li, J.; Yan, D.; Yao, X.; Liu, Y.; Xie, S.; Sheng, Y.; Luan, Z. Carbon Storage Estimation of Coastal Wetlands in China. *Acta Pedol. Sin.* **2022**, *60*, 800–814. [CrossRef]
14. Xiaomin, Z.; Nanshan, Z.; Yun, Q.; Shun, C. Inversing of Vegetation Biomass Based on GPS-R. *Bull. Surv. Mapp.* **2018**, *25*, 129–132. [CrossRef]
15. Cao, L.; Xu, T.; Shen, X. Mapping biomass by integrating Landsat OLI and airborne LiDAR transect data in subtropical forests. *J. Remote Sens.* **2016**, *20*, 665–678.
16. Cui, L.-J.; Ma, Q.-F.; Song, H.-T.; Luan, J.-W. Estimation methods of wetland ecosystem carbon storage: A review. *Chin. J. Ecol.* **2012**, *31*, 2673.
17. Wantai, Y.; Yongqiang, Y. Advances in the research of underground biomass. *Ying Yong Sheng Tai Xue Bao J. Appl. Ecol.* **2001**, *12*, 927–932.
18. Dorrepaal, E.; Cornelissen, J.H.; Aerts, R.; Wallen, B.; Van Logtestijn, R.S. Are growth forms consistent predictors of leaf litter quality and decomposability across peatlands along a latitudinal gradient? *J. Ecol.* **2005**, *93*, 817–828. [CrossRef]
19. Jiao, Y.; Hu, H. Carbon storage and its dynamics of forest vegetations in Heilongjiang Province. *Ying Yong Sheng Tai Xue Bao J. Appl. Ecol.* **2005**, *16*, 2248–2252.
20. Long, Y.; Jiang, F.; Sun, H.; Wang, T.; Zou, Q.; Chen, C. Estimating vegetation carbon storage based on optimal bandwidth selected from geographically weighted regression model in Shenzhen City. *Acta Ecol. Sin.* **2022**, *42*, 4933–4945. [CrossRef]
21. Miao, L.; Guohua, L. Impact factors and uncertainties of the estimation on soil organic carbon storage. *Ecol. Environ. Sci.* **2014**, *23*, 1222–1232.
22. Yin, S.; Yang, Q.; Liu, X. Distribution and accumulation of organic carbon in typical annular wetlands of the Sanjiang Plain. *Chin. J. Soil Sci.* **2006**, *37*, 659–661.
23. Mao, D.; Wang, Z.; Li, L.; Miao, Z.; Ma, W.; Song, C.; Ren, C.; Jia, M. Soil organic carbon in the Sanjiang Plain of China: Storage, distribution and controlling factors. *Biogeosciences* **2015**, *12*, 1635–1645. [CrossRef]
24. Yang, a.; Miao, z.; Qiu, f.; Yang, q.; Wang, z.; Ma, d. A Study on Storage and Distribution of Soil Organic Carbon in SanjiangPlain Based on GIS. *Bull. Soil Water Conserv.* **2015**, *35*, 155–158. [CrossRef]
25. Liu, Y.; Zhang, J.; Zhou, D.; Ma, J.; Dang, R.; Ma, J.; Zhu, X. Temporal and spatial variation of carbon storage in the Shule River Basin based on InVEST model. *Acta Ecol. Sin* **2021**, *41*, 4052–4065.
26. Jiang, W.; Deng, Y.; Tang, Z.; Lei, X.; Chen, Z. Modelling the potential impacts of urban ecosystem changes on carbon storage under different scenarios by linking the CLUE-S and the InVEST models. *Ecol. Model.* **2017**, *345*, 30–40. [CrossRef]
27. Wang, J.; Wu, Y.; Gou, A. Habitat quality evolution characteristics and multi-scenario prediction in Shenzhen based on PLUS and InVEST models. *Front. Environ. Sci.* **2023**, *11*, 210. [CrossRef]
28. Chen, Q.; Xu, X.; Wu, M.; Wen, J.; Zou, J. Assessing the Water Conservation Function Based on the InVEST Model: Taking Poyang Lake Region as an Example. *Land* **2022**, *11*, 2228. [CrossRef]

29. Dan, W.; Wei, H.; Shuwen, Z.; Kun, B.; Bao, X.; Yi, W.; Yue, L. Processes and prediction of land use/land cover changes (LUCC) driven by farm construction: The case of Naoli River Basin in Sanjiang Plain. *Environ. Earth Sci.* **2015**, *73*, 4841–4851. [CrossRef]
30. Mahamat, A.-A.A.; Al-Hurban, A.; Saied, N. Change Detection of Lake Chad Water Surface Area Using Remote Sensing and Satellite Imagery. *J. Geogr. Inf. Syst.* **2021**, *13*, 561–577. [CrossRef]
31. Zhang, Y.; Lei, G.; Zhang, H.; Li, J. Spatiotemporal dynamics of land and water resources matching of cultivated land use based on micro scale in Naoli River Basin. *Trans. Chin. Soc. Agric. Eng.* **2019**, *35*, 185–194.
32. Liu, X.; Li, X.; Liang, X.; Shi, H.; Ou, J. Simulating the change of terrestrial carbon storage in China based on the FLUS-InVEST model. *Trop. Geogr.* **2019**, *39*, 397–409.
33. Qu, C.; Li, W.; Xu, J.; Shi, S. Blackland Conservation and Utilization, Carbon Storage and Ecological Risk in Green Space: A Case Study from Heilongjiang Province in China. *Int. J. Environ. Res. Public Health* **2023**, *20*, 3154. [CrossRef]
34. Zhang, C.; Wang, L.; Song, Q.; Chen, X.; Gao, H.; Wang, X. Biomass carbon stocks and dynamics of forests in Heilongjiang Province from 1973 to 2013. *China Environ. Sci.* **2018**, *38*, 4678–4686.
35. Xu, L.; He, N.; Yu, G. A dataset of carbon density in Chinese terrestrial ecosystems (2010s). *China Sci. Data* **2019**, *4*, 90–96.
36. Yu, R.; Zhao, G.; Chang, C.; Yuan, X.; Wang, Z. Random forest classifier in remote sensing information extraction: A review of applications and future development. *Remote Sens. Infoumation* **2019**, *34*, 8–14.
37. Ning, X.; Chang, W.; Wang, H.; Zhang, H.; Zhu, Q. Extraction of marsh wetland in Heilongjiang Basin based on GEE and multi-source remote sensing data. *Natl. Remote Sens. Bull.* **2022**, *26*, 386–396.
38. López-Tapia, S.; Ruiz, P.; Smith, M.; Matthews, J.; Zercher, B.; Sydorenko, L.; Varia, N.; Jin, Y.; Wang, M.; Dunn, J.B. Machine learning with high-resolution aerial imagery and data fusion to improve and automate the detection of wetlands. *Int. J. Appl. Earth Obs. Geoinf.* **2021**, *105*, 102581. [CrossRef]
39. Bartold, M.; Kluczek, M. A Machine Learning Approach for Mapping Chlorophyll Fluorescence at Inland Wetlands. *Remote Sens.* **2023**, *15*, 2392. [CrossRef]
40. Mainali, K.; Evans, M.; Saavedra, D.; Mills, E.; Madsen, B.; Minnemeyer, S. Convolutional neural network for high-resolution wetland mapping with open data: Variable selection and the challenges of a generalizable model. *Sci. Total Environ.* **2023**, *861*, 160622. [CrossRef]
41. Zi-yun, W.; Jian-wei, L.; Xi, W.; Ying-xin, D.; Tian-liang, W. Degradation Characteristics and Quantitative Research on the Driving Factors of Marshes in Naoli River Basin in Recent 40 Years. *China Rural. Water Hydropower* **2023**, *10*, 47–55. [CrossRef]
42. Liu, J.; Dong, C.; Sheng, L.; Liu, Y. Landscape pattern change of marsh and its response to human disturbance in the small Sanjiang Plain, 1955–2010. *Sci. Geogr. Sin.* **2016**, *36*, 879–887.
43. Hou, W.; Zhang, S.; Zhang, Y.; Kuang, W. Analysis on the shrinking process of wetland in Naoli River Basin of Sanjiang Plain since the 1950s and its driving forces. *J. Nat. Resour.* **2004**, *19*, 725–731.
44. Liu, H.; Zhang, S.; Li, Z.; Lu, X.; Yang, Q. Impacts on wetlands of large-scale land-use changes by agricultural development: The small Sanjiang Plain, China. *AMBIO J. Hum. Environ.* **2004**, *33*, 306–310. [CrossRef]
45. Tang, R.; Peng, K. lmpact of land use change on regional land carbon storage: A review. *Jiangsu Agric. Sci.* **2018**, *46*, 5–11. [CrossRef]
46. Shuqi, L.; Xiaomeng, H.; Yuan, S.; Cai, Y.; Xin, Z. Multi-scenario land use change and its impact on carbon storage based on coupled Plus-Invest model. *Chin. J. Eco-Agric.* **2023**, *31*, 300–314.
47. Chang, S.; Wang, Z.; Song, K. Impact of land use and land cover change on the vegetation carbon storage in Sanjiang Plain. *Ecol. Sci.* **2010**, *29*, 207–214.
48. Wang, L.; Song, C.; Ge, R.; Song, Y.; Liu, D. Soil organic carbon storage under different land-use types in Sanjiang Plain. *China Environ. Sci.* **2009**, *29*, 656–660.
49. Bravo-Martin, S.; Mejías, M.; García-Navarro, F.J.; Jiménez-Ballesta, R. Current status of Las Tablas de Daimiel National Park wetland and actions required for conservation. *Environments* **2019**, *6*, 75. [CrossRef]
50. Chang, X.; Xing, Y.; Wang, J.; Yang, H.; Gong, W. Effects of land use and cover change (LUCC) on terrestrial carbon stocks in China between 2000 and 2018. *Resour. Conserv. Recycl.* **2022**, *182*, 106333. [CrossRef]
51. Maanan, M.; Maanan, M.; Karim, M.; Ait Kacem, H.; Ajrhough, S.; Rueff, H.; Snoussi, M.; Rhinane, H. Modelling the potential impacts of land use/cover change on terrestrial carbon stocks in north-west Morocco. *Int. J. Sustain. Dev. World Ecol.* **2019**, *26*, 560–570. [CrossRef]
52. Zhao, S.; Liu, S.; Sohl, T.; Young, C.; Werner, J. Land use and carbon dynamics in the southeastern United States from 1992 to 2050. *Environ. Res. Lett.* **2013**, *8*, 044022. [CrossRef]